LETTERS

# DAI (DLM-1/ZBP1) is a cytosolic DNA sensor and an activator of innate immune response

Akinori Takaoka[1,3]*, ZhiChao Wang[1]*, Myoung Kwon Choi[1]*, Hideyuki Yanai[1], Hideo Negishi[1], Tatsuma Ban[1], Yan Lu[1], Makoto Miyagishi[2], Tatsuhiko Kodama[5], Kenya Honda[1], Yusuke Ohba[4] & Tadatsugu Taniguchi[1]

**Central to innate immunity is the sensing of pathogen-associated molecular patterns by cytosolic and membrane-associated receptors[1–4]. In particular, DNA is a potent activator of immune responses during infection or tissue damage[5–7], and evidence indicates that, in addition to the membrane-associated Toll-like receptor 9, an unidentified cytosolic DNA sensor(s) can activate type I interferon (IFN) and other immune responses[8–10]. Here we report on a candidate DNA sensor, previously named DLM-1 (also called Z-DNA binding protein 1 (ZBP1))[11], for which biological function had remained unknown; we now propose the alternative name DAI (DNA-dependent activator of IFN-regulatory factors[12]). The artificial expression of otherwise IFN-inducible DAI (DLM-1/ZBP1) in mouse fibroblasts selectively enhances the DNA-mediated induction of type I IFN and other genes involved in innate immunity. On the other hand, RNA interference of messenger RNA for DAI (DLM-1/ZBP1) in cells inhibits this gene induction programme upon stimulation by DNA from various sources. Moreover, DAI (DLM-1/ZBP1) binds to double-stranded DNA and, by doing so, enhances its association with the IRF3 transcription factor and the TBK1 serine/threonine kinase. These observations underscore an integral role of DAI (DLM-1/ZBP1) in the DNA-mediated activation of innate immune responses, and may offer new insight into the signalling mechanisms underlying DNA-associated antimicrobial immunity and autoimmune disorders.**

Nucleic acids, exposed in a cell by infection or by incomplete clearance during cell damage, can evoke immune responses[6,13,14]. In addition to RNA-sensing mechanisms[4,15–19], recent attention has focused on characterizing DNA-sensing systems as they also evoke protective and pathological immune responses. Evidence indicates the presence of a cytosolic DNA sensor(s) that can initiate innate immune responses, including the induction of type I IFN genes[8,9,20], independently of Toll-like receptor 9 (TLR9), the membrane

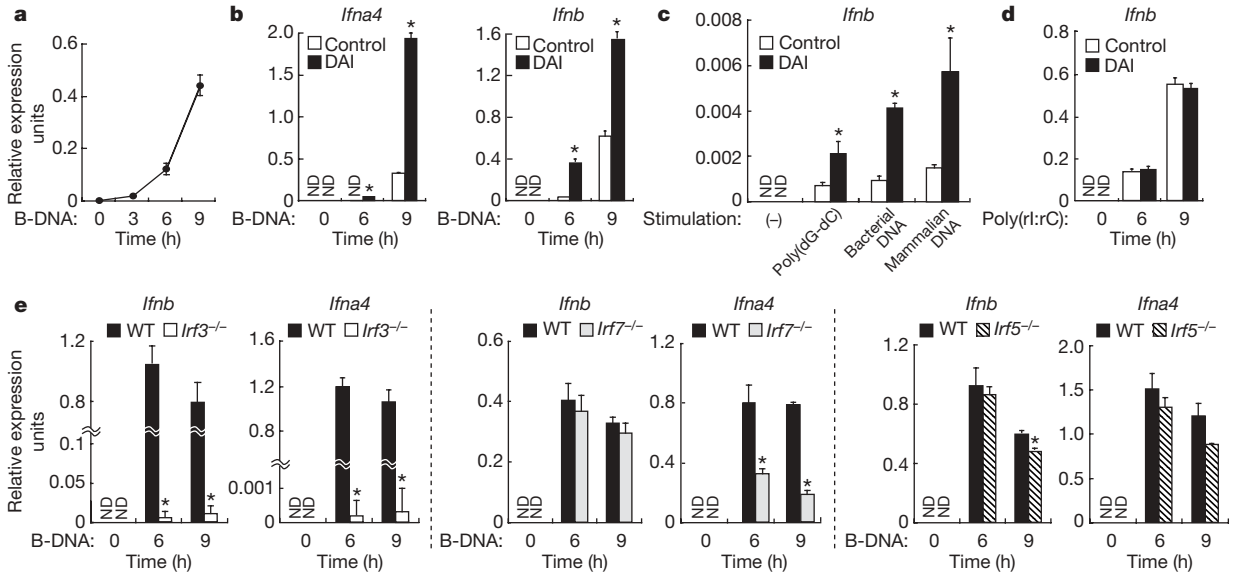


**Figure 1 | DAI (DLM-1/ZBP1) is a positive regulator for type I IFN induction by cytosolic DNA. a**, Induction of *DAI* (*DLM-1/Zbp1*) mRNA by poly(dA-dT)•poly(dT-dA) (B-DNA) in MEFs was analysed by quantitative RT–PCR. Error bars in all panels indicate s.d. ($n = 3$). **b–d**, L929 fibroblasts retrovirally expressing mock (control) or DAI (DLM-1/ZBP1) were treated with B-DNA (**b**), poly(dG-dC)•poly(dC-dG) and bacterial (*Escherichia coli*) or mammalian (calf thymus) genomic DNAs (**c**), or poly(rI:rC) (**d**), and then assayed for IFN-α/β mRNAs by quantitative RT–PCR. Similarly, an enhanced effect by DAI (DLM-1/ZBP1) expression was observed in MEFs (Supplementary Fig. 1g). Asterisk, $P < 0.01$, DAI (DLM-1/ZBP1) versus control. ND, not detected. **e**, Wild-type (WT) and littermate *Irf3*$^{-/-}$, *Irf7*$^{-/-}$ and *Irf5*$^{-/-}$ MEFs were treated with B-DNA, and then assessed for the expression of IFN-α/β mRNAs by quantitative RT–PCR. Asterisk, $P < 0.01$ as compared with wild-type MEFs.

[1]Department of Immunology, and [2]Department of 21st Century Center of Excellence Program, Graduate School of Medicine and Faculty of Medicine, University of Tokyo, Hongo 7-3-1, Bunkyo-ku, Tokyo 113-0033, Japan. [3]Division of Signaling in Cancer and Immunology, Institute for Genetic Medicine, Hokkaido University, and [4]Department of Laboratory Medicine, Hokkaido University Graduate School of Medicine, N15, W7, Kita-ku, Sapporo 060-0815, Japan. [5]Department of Molecular Biology and Medicine, Research Center for Advanced Science and Technology, University of Tokyo, Komaba 4-6-1, Meguro-ku, Tokyo 153-8904, Japan.
*These authors contributed equally to this work.

receptor activated by hypomethylated DNA[5,20]. We came across an IFN-inducible gene that piqued our interest for its potential role in DNA sensing (Supplementary Fig. 1a–c)—this gene was first identified in tumour stromal tissue and named *DLM-1* (ref. 11), and was later reported to contain two binding domains for left-handed Z-form DNA (Z-DNA) and hence was also termed *Zbp1* (refs 21, 22). Nevertheless, neither a rigorous assessment of its biological function nor its ability to interact with other DNA was performed.

As shown in Fig. 1a and Supplementary Fig. 1d, mRNA expression for *DLM-1*/*Zbp1* is strongly upregulated in mouse embryonic fibroblasts (MEFs) and L929 cells when stimulated with a synthetic DNA, poly(dA-dT)•poly(dT-dA), which may take on a B-form configuration in solution and strongly evoke innate immune responses[9] (hereafter referred to as B-DNA for convenience; see Methods). This gene induction is dependent on type I IFN signalling (Supplementary Fig. 1e; see also ref. 9). Many genes involved in stimulating IFN responses, including those for cytosolic RNA sensors[15,16], are themselves IFN-inducible; this positive feedback regulation thereby ensures a robust innate immune response. Thus, we hypothesized that DLM-1/ZBP1 may function in the DNA-mediated activation of innate immunity. In light of its newly revealed function demonstrated below, we propose the alternative name of DAI (DNA-dependent activator of IFN-regulatory factors), although we use DAI (DLM-1/ZBP1) throughout for continuity and to acknowledge previous publications.

To assess the contribution of DAI (DLM-1/ZBP1) to a DNA-mediated immune response, we artificially expressed DAI (DLM-1/ZBP1) cDNA in L929 cells (Supplementary Fig. 1f), stimulated the cells with B-DNA, and then examined type I IFN gene induction. As shown in Fig. 1b, B-DNA-induced expression of IFN-α (α4) and IFN-β mRNAs (*Ifna4* and *Ifnb*, respectively) occurred much earlier and reached a higher level in DAI (DLM-1/ZBP1)-expressing L929 cells than in control cells. This DAI (DLM-1/ZBP1)-mediated response was dose dependent (Supplementary Fig. 2a, b) and probably TLR9-independent (refs 9, 10; see also Supplementary Fig. 3a, b). Notably, enhancement of *Ifnb* mRNA induction in DAI (DLM-1/ZBP1)-expressing L929 cells was also observed upon treatment with bacteria- and calf-thymus-derived DNA as well as with a synthetic poly(dG-dC)•poly(dC-dG) DNA that may take on a Z-form

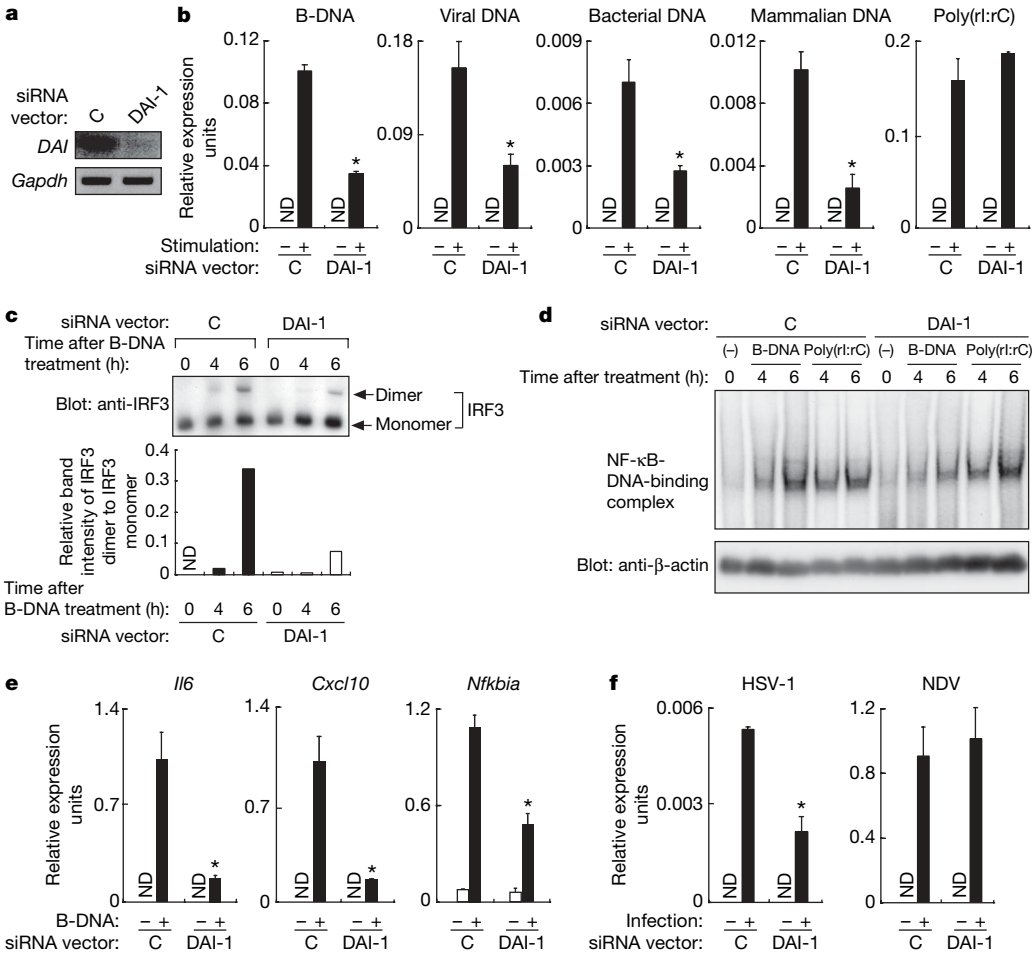


**Figure 2 | DAI (DLM-1/ZBP1) is critical for B-DNA-mediated IRF3 activation and *Ifnb* mRNA expression.** **a**, L929 cells were transfected with a plasmid vector encoding a control siRNA (C) or *DAI* (*DLM-1/Zbp1*)-targeting siRNA (DAI-1), and subjected to RT–PCR analysis to evaluate the expression of *DAI* (*DLM-1/Zbp1*) and *Gapdh* mRNA. **b**, The induction of *Ifnb* mRNA in siRNA-expressing L929 cells was measured by quantitative RT–PCR upon treatment with B-DNA, viral (vaccinia virus), bacterial (*E.coli*) or mammalian (calf thymus) genomic DNAs, or poly(rI:rC). Data are mean ± s.d. ($n = 3$). Asterisk, $P < 0.01$, siRNA-DAI-1 versus siRNA-C. ND, not detected. The protein levels of IFN-β were also evaluated by ELISA (Supplementary Fig. 7e). **c**, B-DNA-induced dimerization of IRF3 in siRNA-expressing L929 cells. The relative band intensities of IRF3 dimer quantified by a densitometer were normalized to those of IRF3 monomer, and depicted in graphs (bottom). **d**, B-DNA- or poly(rI:rC)-induced activation of NF-κB in siRNA-expressing L929 cells was analysed by EMSA. Immunoblots with anti-β-actin from a parallel set of identical samples is also shown as a loading control (bottom panel). **e**, B-DNA-induced expression of *Il6*, *Cxcl10* and *Nfkbia* mRNAs in siRNA-expressing L929 cells was assessed by quantitative RT–PCR. Data are mean ± s.d. ($n = 3$). Asterisk, $P < 0.01$, siRNA-DAI-1 versus siRNA-C. The protein levels of these cytokines were also evaluated by ELISA (Supplementary Fig. 7e). **f**, The induction of *Ifnb* mRNA by HSV-1 (left panel) or NDV (right) was examined in siRNA-expressing L929 cells by quantitative RT–PCR. Data are mean ± s.d. ($n = 3$). Asterisk, $P < 0.01$, siRNA-DAI-1 versus siRNA-C.

configuration[23] (Fig. 1c). On the other hand, such an enhancement was not made when these cells were stimulated with poly(rI:rC), a synthetic double-stranded RNA that activates the RIG-I/MDA5 cytosolic pathway (Fig. 1d and Supplementary Fig. 2a; see also refs 15, 16). Consistent with these findings, in MEFs deficient for IFN-α/β receptor subunit 1 (*Ifnar1*)—in which impaired *Ifnb* mRNA induction by B-DNA stimulation (Supplementary Fig. 4a) is presumably due, in part, to the failure to induce DAI (DLM-1/ZBP1)—exogenous DAI (DLM-1/ZBP1) expression resulted in the rescue of *Ifnb* mRNA induction in response to DNA, but not to RNA (Supplementary Fig. 4b, c). The B-DNA-mediated induction of mRNAs for other DNA-inducible genes[9,10] involved in innate immunity was also upregulated in DAI (DLM-1/ZBP1)-expressing L929 cells (Supplementary Fig. 5a, b).

Whereas IFN-regulatory factor 3 (IRF3) is critical to the cytosolic DNA-mediated induction of IFN genes, the contribution of other IRFs has not been examined. Therefore, we next examined the induction of IFN genes upon B-DNA stimulation in MEFs derived from mice deficient in one of three IRFs (*Irf3*$^{-/-}$, *Irf7*$^{-/-}$ or *Irf5*$^{-/-}$ MEFs; refs 24–26). As shown in Fig. 1e, B-DNA-mediated *Ifnb* mRNA induction was abolished in *Irf3*$^{-/-}$ MEFs, but was similar to wild-type levels in *Irf7*$^{-/-}$ and *Irf5*$^{-/-}$ MEFs. On the other hand, the induction of *Ifna4* mRNA was impaired in *Irf7*$^{-/-}$ MEFs, suggesting that IRF7 cooperates with IRF3 in the activation of this (and possibly other) IFN-α gene subtype (Fig. 1e). Because the effect of DAI (DLM-1/ZBP1) was observed in wild-type MEFs (Supplementary Fig. 1g) but not in *Irf3*$^{-/-}$ or *Irf7*$^{-/-}$ MEFs (Supplementary Fig. 6), we presume that these transcription factors function downstream of DAI (DLM-1/ZBP1).

We next used a small interfering RNA (siRNA) to knockdown *DAI* (*DLM-1/Zbp1*) mRNA levels and then examined the activation of IFN and other genes involved in innate immune responses. The siRNA-DAI-1 construct strongly knocked down endogenous *DAI* (*DLM-1/Zbp1*) mRNA (Fig. 2a) and its protein (Z.W., unpublished data) in L929 cells and effectively suppressed the levels of an artificially expressed DAI (DLM-1/ZBP1) protein in HEK293T cells (Supplementary Fig. 7a). Notably, the induction of *Ifnb* and *Ifna4* mRNAs by B-DNA as well as by viral, bacterial or mammalian DNA was strongly inhibited in cells expressing siRNA-DAI-1, but not in cells expressing a control siRNA vector (siRNA-C) (Fig. 2b and data not shown). Induction of *Ifnb* mRNA upon poly(rI:rC) stimulation, however, was not affected by siRNA-DAI-1 expression (Fig. 2b and Supplementary Fig. 7b). Similar observations were made in the macrophage cell line RAW264.7 when transfected with the same siRNA vectors (Supplementary Fig. 7c) and in L929 cells transfected with siRNA-DAI-2, an siRNA vector targeted to a different region of *DAI* (*DLM-1/Zbp1*) mRNA (Supplementary Fig. 7d). Consistent with these data, B-DNA-induced dimerization of IRF3 was inhibited by approximately fourfold in siRNA-DAI-1-expressing L929 cells (Fig. 2c). Notably, the DNA-mediated activation of NF-κB was also inhibited in siRNA-DAI-1-expressing cells (Fig. 2d), as was the induction of NF-κB-dependent genes and their products (Fig. 2e and Supplementary Fig. 7e). Therefore, DAI (DLM-1/ZBP1) may also be involved in the DNA-mediated activation of the NF-κB pathway, although we cannot exclude the possibility that a DNA sensor(s) other than DAI (DLM-1/ZBP1) is also involved.

Consistent with the notion that DAI (DLM-1/ZBP1) is involved in DNA-mediated antiviral responses through type I IFN induction, siRNA-DAI-1-expressing cells were found to be more sensitive to virus infection than siRNA-C-expressing cells after B-DNA stimulation (Supplementary Fig. 8). To address this issue further, we next measured the effect of siRNA-DAI-1 expression on the induction of *Ifnb* mRNA in response to infection by a DNA virus, herpes simplex virus-1 (HSV-1), or an RNA virus, Newcastle disease virus (NDV). As shown in Fig. 2f, induction of *Ifnb* mRNA was inhibited, albeit not completely, when siRNA-DAI-1-expressing L929 cells were infected by HSV-1, but not by NDV. Furthermore, the HSV-1 yield was notably higher (between five- and sixfold) in

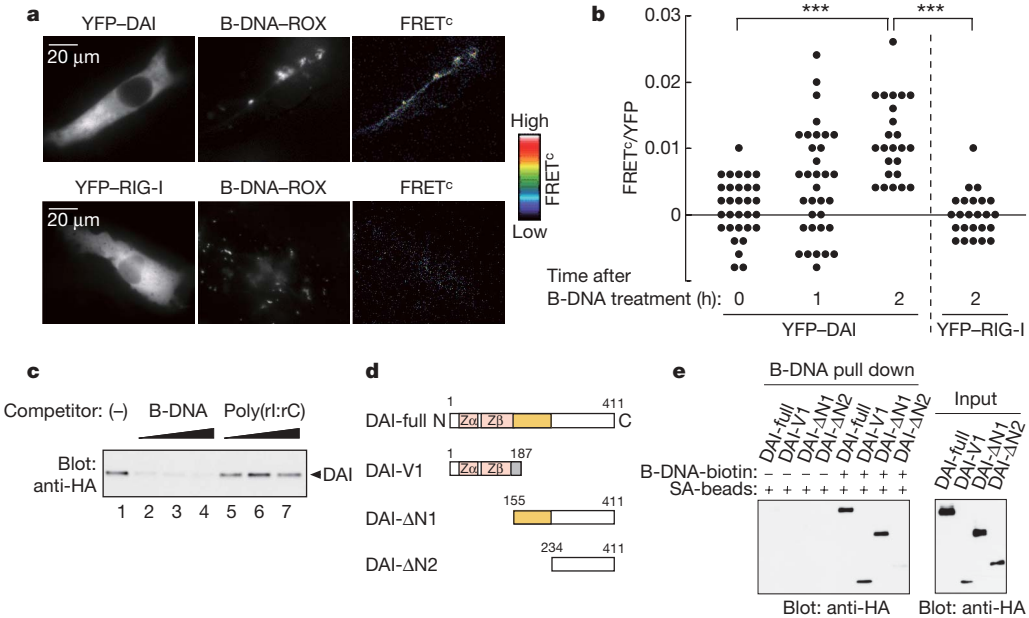


**Figure 3 | Interaction of DAI (DLM-1/ZBP1) with B-DNA in the cytoplasm.** **a**, **b**, Intermolecular FRET analysis for the interaction between DAI (DLM-1/ZBP1) and B-DNA. HeLa cells expressing YFP-tagged DAI (DLM-1/ZBP1) (top row) or YFP-tagged RIG-I (bottom row) were stimulated for 2 h with rhodamine (ROX)-conjugated B-DNA and then analysed by fluorescence microscopy. Representative fluorescence images of YFP, ROX and FRET$^{C}$ (corrected FRET; displayed in pseudo-colour mode) are shown from left to right (**a**). FRET$^{C}$/YFP values were calculated and plotted as a histogram (**b**). Triple asterisk, $P < 0.0001$. **c**, Pull-down assays were performed with whole-cell lysates from HA–DAI (DLM-1/ZBP1)-expressing HEK293T cells in the absence ((−); lane 1) of or after pre-incubation with unconjugated B-DNA (lanes 2–4) or poly(rI:rC) (lanes 5–7; 5.0, 10, 20 μg ml$^{-1}$; wedges). Bound proteins were analysed by immunoblotting with anti-HA antibody. **d**, **e**, A pull-down assay was performed for the HA-tagged full length of DAI (DLM-1/ZBP1) (DAI-full) and three deletion mutant proteins (illustrated in **d**; numbers denote the residue numbers), as described in **c**. The domain in yellow corresponds to the D3 region (see text for details). Input protein levels for this assay are shown. Quantitative analysis of the levels of pulled-down proteins is shown in Supplementary Fig. 11. Zα and Zβ indicate the N-terminal Z-DNA binding domains. SA, streptavidin.

siRNA-DAI-1-expressing cells as compared to control cells 12 h after viral infection (Supplementary Fig. 9a), whereas there was no such increase upon NDV infection (Supplementary Fig. 9b), further supporting the view that DAI (DLM-1/ZBP1) selectively contributes to HSV-1-mediated type I IFN gene induction and antiviral immune response. The mechanisms for sensing DNA viruses are, nevertheless, likely to involve additional molecules and complexities.

To examine the interaction between DNA and DAI (DLM-1/ZBP1), we next performed fluorescence resonance energy transfer (FRET) analysis in HeLa cells using B-DNA labelled with rhodamine (ROX), and DAI (DLM-1/ZBP1) or RIG-I each tagged with yellow fluorescent protein (YFP). As shown in Fig. 3a, b, a FRET signal was observed only between B-DNA and DAI (DLM-1/ZBP1), demonstrating that DNA is in selective and direct contact with DAI (DLM-1/ZBP1). DAI (DLM-1/ZBP1) mainly resides in the cytosol with a diffuse but partially granular-like pattern in HeLa cells and L929 cells (Fig. 3a and Supplementary Fig. 10a; see also refs 27, 28). We next studied the interaction of DAI (DLM-1/ZBP1) with B-DNA by co-precipitation assay. Protein lysates from HEK293T cells transiently expressing haemagglutinin (HA)-tagged DAI (DLM-1/ZBP1) or the transcription factor Stat1, used as a control, were subjected to a 'pull-down assay' with biotin-labelled B-DNA and streptavidin-conjugated magnetic beads. As shown in Fig. 3c and Supplementary Fig. 10b, DAI (DLM-1/ZBP1), but not Stat1, precipitated with the DNA. This precipitation was inhibited by an excess amount of non-conjugated B-DNA, but not poly(rI:rC). Thus, DAI (DLM-1/ZBP1) may selectively and directly interact with B-DNA, although it cannot be excluded that other intermediate protein(s) may also participate in this intermolecular interaction.

To determine the region(s) of DAI (DLM-1/ZBP1) involved in this interaction, we constructed a series of complementary DNA expression vectors each encoding a deletion mutant of DAI (DLM-1/ZBP1) (Fig. 3d), expressed them in HEK293T cells, and then performed the co-precipitation assay. As shown in Fig. 3e, the DAI-V1 and DAI-ΔN1 mutants precipitated with the conjugated B-DNA, whereas DAI-ΔN2 failed to do so. Thus, in addition to the previously determined DNA-binding domains[22], another region tentatively denoted as the D3 region (Fig. 3d, yellow) may also participate in the interaction with DNA. A more detailed analysis, however, will be required to determine whether this interaction is direct or indirect and which of the DNA-binding regions are critical for the activation of DAI (DLM-1/ZBP1) in response to a given DNA stimulus. It is intriguing that a variety of DNA, be it synthetic DNA or DNA of bacterial, viral or mammalian origin, activate DAI (DLM-1/ZBP1), albeit with different efficiencies (Figs 1c and 2b). Thus, we infer that DAI (DLM-1/ZBP1) activation by and discrimination between B- and Z-form and host- and pathogen-derived DNA may not be absolutely stringent. Rather, DAI (DLM-1/ZBP1) activation is also likely to be a function of the quantitative amount and the length of the DNA in the cytosol.

Because TBK1 is essential for the DNA-induced activation of IRF3 (ref. 9), we further analysed the molecular association of DAI (DLM-1/ZBP1) with TBK1 and IRF3 by assaying for the co-immunoprecipitation of HA-tagged DAI (DLM-1/ZBP1) with Flag-tagged TBK1 or IRF3 in L929 cells. As shown in Fig. 4a, DAI (DLM-1/ZBP1) co-precipitated with both TBK1 and IRF3, maximally, 2 h after B-DNA stimulation, suggesting that DAI (DLM-1/ZBP1) associates, either directly or indirectly, with TBK1 and IRF3 and that this association is enhanced upon cytosolic DNA stimulation of cells. We therefore postulate that when TBK1 and IRF3 are recruited to the DNA–DAI (DLM-1/ZBP1) complex, IRF3 is activated and undergoes nuclear translocation and, in the absence of IRF3, TBK1 dissociates from the complex. Although further work will be required, this notion is consistent with our preliminary observations that indicate the nuclear translocation of IRF3 after its dissociation from DNA–DAI (DLM-1/ZBP1) (data not shown). To determine which region of DAI (DLM-1/ZBP1) is necessary for its interaction with TBK1 and IRF3, HA-tagged deletion mutants of DAI

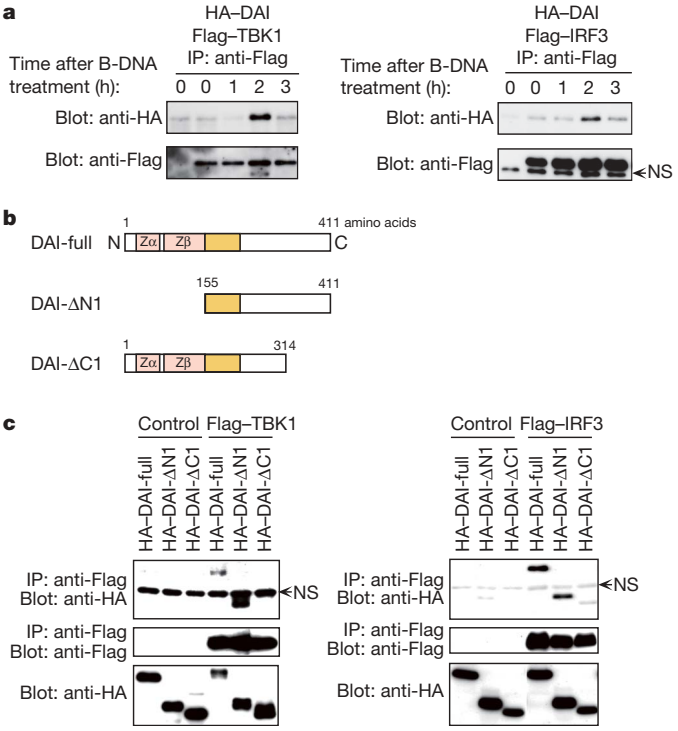


**Figure 4 | Interaction of DAI (DLM-1/ZBP1) with IRF3 and TBK1. a**, L929 cells transiently expressing HA–DAI (DLM-1/ZBP1) together with Flag–TBK1 (left panel) or Flag–IRF3 (right panel) were stimulated with B-DNA and analysed by immunoprecipitation with anti-Flag antibody, followed by immunoblotting with anti-HA (top panel) and anti-Flag (bottom panel) antibodies. The first lane of each panel shows the results of cells expressing HA–DAI (DLM-1/ZBP1) alone. NS, nonspecific bands. **b**, **c**, Full-length DAI (DLM-1/ZBP1) or two deletion mutants (illustrated in **b**) were transiently expressed in HEK293T cells alone (control) or along with either Flag–TBK1 (left panel) or Flag–IRF3 (right panel). Cell lysates were analysed as described in **a**. DAI (DLM-1/ZBP1) can be readily co-immunoprecipitated by these proteins even without DNA stimulation, presumably because of its high level of protein expression in HEK293T cells.

(DLM-1/ZBP1) were co-expressed with Flag-tagged TBK1 or IRF3 in HEK293T cells (Fig. 4b). As shown in Fig. 4c, interaction of DAI-ΔN1 but not DAI-ΔC1 with TBK1 and IRF3 was observed, suggesting that the ~100 carboxy-terminal amino acids of DAI (DLM-1/ZBP1) are critical for its intermolecular associations.

Our present study reveals that DAI (DLM-1/ZBP1) is a cytoplasmic recognition receptor that senses and is activated by DNA from a variety of sources, leading to type I IFN gene induction through the activation of IRF3 and, probably, IRF7. Notably, this sensor may itself recruit IRF3 and TBK1 in a DNA-dependent manner, although additional experiments will be required to confirm the formation of this signalling complex. Thus, unlike the RNA sensor RIG-I, which becomes constitutively active in the absence of its RNA interaction region (ref. 15), DAI (DLM-1/ZBP1) may require both its amino-terminal DNA-binding region and carboxy-terminal TBK1/IRF binding region for its activity. Therefore, DNA is not only critical to initiate but also to sustain the active signalling complex. Consistent with this notion, neither DAI-ΔN2 lacking the DNA-binding region nor DAI-ΔC1 lacking the TBK1/IRF recruiting region can mediate DNA-stimulated *Ifnb* mRNA induction (Supplementary Fig. 12).

The rigorous examination to determine the extent to which DAI (DLM-1/ZBP1) contributes to the cytosolic DNA-mediated and/or virus-mediated activation of innate immune responses must await the generation of mice deficient in the corresponding gene. The mutant mice will permit the study of DAI (DLM-1/ZBP1)'s function in distinct cell types *in vitro* and *in vivo* in the context of protective and pathological immune responses.

## METHODS SUMMARY

**Mice, cells and reagents.** The generation of *Irf3*$^{-/-}$, *Irf5*$^{-/-}$ and *Irf7*$^{-/-}$ mice has been described previously[24–26]. MEFs were prepared and murine L929 fibroblasts were cultured as described previously[24]. Details of nucleic acid ligands and other reagents are described in the Methods.

**Viral infection.** Cells were infected for 12 h with 1.0 multiplicity of infection (M.O.I.) of HSV-1 (KOS strain; VR-1493; ATCC) or 25 haemagglutinin units (HAU) of NDV, as described previously[24].

**Plasmids and gene transfer.** Details of plasmid construction are described in the Methods. Retroviral gene transfer or transfection by electroporation was carried out as described previously[24,26]. Briefly, two days after infection with retrovirus, cells were selected with puromycin (3.0 μg ml$^{-1}$) for 2 days, and used for further experiments.

**RNA analysis.** RNA extraction and RT–PCR were performed as described previously[26]. The primers used in quantitative RT–PCR analysis are described in the Methods. Details of RNA interference are described in the Methods.

**Electrophoretic mobility shift assay (EMSA).** EMSA was performed as described previously[26], and the protocol is briefly described in the Methods.

**Fluorescence microscopy.** These analyses including FRET were carried out as described previously[26], and are briefly mentioned in the Methods.

**Pull-down assay.** This assay was performed with a synthetic, biotin-conjugated poly(dA-dT)•poly(dT-dA) and streptavidin-conjugated magnetic beads (Dynal Biotech). The details are described in the Methods.

**Immunoprecipitation and immunoblotting.** Cell lysis, co-immunoprecipitation and immunoblotting were carried out as described previously[26]. IRF3 dimer was assessed by native PAGE, followed by immunoblotting with anti-mouse IRF3 antibody, as described previously[15]. The quantification of IRF3 dimer was performed by the NIH Image application. Similar results were obtained in three independent transfection experiments.

**Full Methods** and any associated references are available in the online version of the paper at www.nature.com/nature.

**Received 13 March; accepted 13 June 2007.**
**Published online 8 July 2007.**

1. Janeway, C. A. Jr & Medzhitov, R. Innate immune recognition. *Annu. Rev. Immunol.* **20,** 197–216 (2002).
2. Takeda, K., Kaisho, T. & Akira, S. Toll-like receptors. *Annu. Rev. Immunol.* **21,** 335–376 (2003).
3. Meylan, E., Tschopp, J. & Karin, M. Intracellular pattern recognition receptors in the host response. *Nature* **442,** 39–44 (2006).
4. Creagh, E. M. & O'Neill, L. A. TLRs, NLRs and RLRs: a trinity of pathogen sensors that co-operate in innate immunity. *Trends Immunol.* **27,** 352–357 (2006).
5. Krieg, A. M. *et al.* CpG motifs in bacterial DNA trigger direct B-cell activation. *Nature* **374,** 546–549 (1995).
6. Tokunaga, T., Yamamoto, T. & Yamamoto, S. How BCG led to the discovery of immunostimulatory DNA. *Jpn. J. Infect. Dis.* **52,** 1–11 (1999).
7. Ishii, K. J. & Akira, S. Innate immune recognition of, and regulation by, DNA. *Trends Immunol.* **27,** 525–532 (2006).
8. Hochrein, H. *et al.* Herpes simplex virus type-1 induces IFN-α production via Toll-like receptor 9-dependent and -independent pathways. *Proc. Natl Acad. Sci. USA* **101,** 11416–11421 (2004).
9. Ishii, K. J. *et al.* A Toll-like receptor-independent antiviral response induced by double-stranded B-form DNA. *Nature Immunol.* **7,** 40–48 (2006).
10. Stetson, D. B. & Medzhitov, R. Recognition of cytosolic DNA activates an IRF3-dependent innate immune response. *Immunity* **24,** 93–103 (2006).
11. Fu, Y. *et al.* Cloning of DLM-1, a novel gene that is up-regulated in activated macrophages, using RNA differential display. *Gene* **240,** 157–163 (1999).
12. Honda, K. & Taniguchi, T. IRFs: master regulators of signalling by Toll-like receptors and cytosolic pattern-recognition receptors. *Nature Rev. Immunol.* **6,** 644–658 (2006).
13. Napirei, M. *et al.* Features of systemic lupus erythematosus in Dnase1-deficient mice. *Nature Genet.* **25,** 177–181 (2000).
14. Yoshida, H., Okabe, Y., Kawane, K., Fukuyama, H. & Nagata, S. Lethal anemia caused by interferon-β produced in mouse embryos carrying undigested DNA. *Nature Immunol.* **6,** 49–56 (2005).
15. Yoneyama, M. *et al.* The RNA helicase RIG-I has an essential function in double-stranded RNA-induced innate antiviral responses. *Nature Immunol.* **5,** 730–737 (2004).
16. Kato, H. *et al.* Differential roles of MDA5 and RIG-I helicases in the recognition of RNA viruses. *Nature* **441,** 101–105 (2006).
17. Alexopoulou, L., Holt, A. C., Medzhitov, R. & Flavell, R. A. Recognition of double-stranded RNA and activation of NF-κB by Toll-like receptor 3. *Nature* **413,** 732–738 (2001).
18. Hornung, V. *et al.* 5′-Triphosphate RNA is the ligand for RIG-I. *Science* **314,** 994–997 (2006).
19. Pichlmair, A. *et al.* RIG-I-mediated antiviral responses to single-stranded RNA bearing 5′-phosphates. *Science* **314,** 997–1001 (2006).
20. Verthelyi, D. & Zeuner, R. A. Differential signaling by CpG DNA in DCs and B cells: not just TLR9. *Trends Immunol.* **24,** 519–522 (2003).
21. Ha, S. C. *et al.* Biochemical characterization and preliminary X-ray crystallographic study of the domains of human ZBP1 bound to left-handed Z-DNA. *Biochim. Biophys. Acta* **1764,** 320–323 (2006).
22. Schwartz, T., Behlke, J., Lowenhaupt, K., Heinemann, U. & Rich, A. Structure of the DLM-1–Z-DNA complex reveals a conserved family of Z-DNA-binding proteins. *Nature Struct. Biol.* **8,** 761–765 (2001).
23. Rich, A. & Zhang, S. Timeline: Z-DNA: the long road to biological function. *Nature Rev. Genet.* **4,** 566–572 (2003).
24. Sato, M. *et al.* Distinct and essential roles of transcription factors IRF-3 and IRF-7 in response to viruses for IFN-α/β gene induction. *Immunity* **13,** 539–548 (2000).
25. Honda, K. *et al.* IRF-7 is the master regulator of type-I interferon-dependent immune responses. *Nature* **434,** 772–777 (2005).
26. Takaoka, A. *et al.* Integral role of IRF-5 in the gene induction programme activated by Toll-like receptors. *Nature* **434,** 243–249 (2005).
27. Deigendesch, N., Koch-Nolte, F. & Rothenburg, S. ZBP1 subcellular localization and association with stress granules is controlled by its Z-DNA binding domains. *Nucleic Acids Res.* **34,** 5007–5020 (2006).
28. Pham, H. T., Park, M. Y., Kim, K. K., Kim, Y. G. & Ahn, J. H. Intracellular localization of human ZBP1: Differential regulation by the Z-DNA binding domain, Zα, in splice variants. *Biochem. Biophys. Res. Commun.* **348,** 145–152 (2006).

**Supplementary Information** is linked to the online version of the paper at www.nature.com/nature.

**Acknowledgements** We thank A. Katoh and M. Kidokoro for the vaccinia virus (MO) genome for ligand stimulation; T. Fujita and M. Yoneyama for RIG-I cDNA; J. Miyazaki for pCAGGS; A. Miyawaki for Venus; R. Kuroda for her support for CD spectrometry; Toray Industries for murine IFN-β; J. V. Ravetch for advice; Y. Fujita, R. Takeda and M. Shishido for technical assistance; and D. Savitsky for critical reading of the manuscript. This work was supported in part by a grant for Advanced Research on Cancer and a Grant-In-Aid for Scientific Research on Priority Areas, and for Scientific Research, from the Ministry of Education, Culture, Sports, Science, and Technology of Japan. Z.W. and H.N. are research fellows of the Japan Society for the Promotion of Science. M.K.C. is a research fellow of the Korea Science and Engineering Foundation.

**Author Contributions** A.T., Z.W., M.K.C., H.Y., H.N., T.B., Y.L. and T.T. conceived the research, planned experiments and analyses, and largely conducted experiments. K.H. and M.M. helped to design RNAi experimental protocols. T.K. performed microarray experiments and data analysis. Fluorescence microscopy and FRET analysis were conducted by Y.O. T.T. oversaw the entire project.

**Author Information** Reprints and permissions information is available at www.nature.com/reprints. The authors declare no competing financial interests. Correspondence and requests for materials should be addressed to T.T. (tada@m.u-tokyo.ac.jp).

## METHODS

**Mice, cells and reagents.** All mice used for this study were backcrossed to the C57BL/6 background. Poly(dA-dT)•poly(dT-dA), poly(dG-dC)•poly(dC-dG) and calf thymus genomic DNA were purchased from Sigma. There is an abundance of literature showing that poly(dA-dT)•poly(dT-dA) can adopt non-B-DNA conformations including left-handed Z-DNA[29]. We confirmed by circular dichroism (CD) analysis that poly(dA-dT)•poly(dT-dA) adopts a B-conformation in solution, and that the transfection reagent Lipofectamine2000 does not induce Z-conformation of the DNA (data not shown), as previously described[9,30]. Therefore, we expediently used the term B-DNA for poly(dA-dT)•poly(dT-dA) for convenience as a ligand for stimulation, although it currently remains unclear whether the poly(dA-dT)•poly(dT-dA) used in our study is indeed in a B-conformation during its interaction with DAI (DLM-1/ZBP1). Rhodamine (ROX)- and biotin-conjugated poly(dA-dT)•poly(dT-dA) were purchased from Hokkaido System Science. Purified vaccinia virus (MO) DNA was provided by A. Kato and M. Kidokoro. *Escherichia coli* DNA and poly(rI:rC) were purchased from InvivoGen and Amersham Biosciences, respectively. B-DNA or poly(rI:rC) was used at a concentration of 6.0 μg ml$^{-1}$ or 5.0 μg ml$^{-1}$, respectively, unless otherwise mentioned. Other nucleic acid ligands were used at 10.0 μg ml$^{-1}$ following complex formation with Lipofectamine2000 (Invitrogen) at a ratio of 1.0 μl lipofectamine to 1.0 μg DNA in OptiMEM (Invitrogen). Antibodies against the following proteins were purchased from the vendors indicated: IRF3 (ZM3; Zymed), β-actin (AC-15; Sigma-Aldrich), HA (3F10; Roche), Flag (M2; Sigma), NFκB p65 (C20; Santa Cruz Biotechnology).

**Plasmid constructions.** HA–IRF3 expression vector has been described previously[26]. Mouse *DAI* (*DLM-1/Zbp1*) cDNA was obtained by polymerase chain reaction with reverse transcription (RT–PCR) on total RNA from splenocytes, and then cloned into the pT7Blue vector (Novagen). To generate YFP-, Flag- and HA-tagged DAI (DLM-1/ZBP1) expression vectors, the *DAI* (*DLM-1/Zbp1*) cDNA was cloned into the *Xho*I and *Not*I sites of the pCAGGS-YFP, pCXN2-Flag and pCAGGS-HA vectors. Flag–IRF3 and Flag–TBK1 expression vectors were generated by subcloning the respective cDNAs into the same sites of pCXN2-Flag. The pCAGGS vector and Venus, which we refer to as YFP, were provided by J. Miyazaki and A. Miyawaki, respectively. To generate the DAI (DLM-1/ZBP1) retroviral expression vector, *DAI* (*DLM-1/Zbp1*) cDNA was excised from pCAGGS-HA- DAI (DLM-1/ZBP1) and cloned into the *Sal*I and *Not*I sites of the MSCVpac-Flag. A splicing variant DAI-V1 (1–187 amino acids) and other deletion mutants (DAI-ΔN1 (155–411), DAI-ΔN2 (234–411) and DAI-ΔC1 (1–314)) were isolated by PCR and inserted into the *Xho*I and *Not*I sites of pCAGGS-HA. Each cDNA of DAI-ΔN2 or DAI-ΔC1 was excised from pCAGGS-HA-DAI and cloned into the *Sal*I and *Not*I sites of MSCVpac-Flag. As shown in Fig. 3d, DAI-V1 is a naturally occurring splice variant that encodes a truncated protein containing 36 unique amino acids at its carboxy terminus (grey; Ensembl Gene ID ENSMUSESTT00003754309). DAI-ΔN1 is lacking both of the N-terminal Z-DNA binding domains (Zα and Zβ), whereas DAI-ΔN2 is missing the D3 region as well as both of the Z-DNA binding domains. RIG-I cDNA was provided by T. Fujita and M. Yoneyama. YFP-tagged RIG-I was generated by subcloning RIG-I cDNA into the *Xho*I and *Not*I sites of the pCAGGS-YFP expression vector.

**Quantitative RT–PCR analysis.** This analysis was performed with a Lightcycler480 and SYBR Green system (Roche Molecular Biochemicals). All data were presented as relative expression units after normalization to *Gapdh*. Primer sequences for murine *DAI* (*DLM-1/Zbp1*), *Ccl5* and *Cxcl10* are as follows: *DAI* sense 5′-GACGACAGCCAAAGAAGTGA-3′; *DAI* antisense 5′-GAGCTATGTCTTGGCCTTCC-3′; *Ccl5* sense 5′-ACGTCAAGGAGTATTTCTACAC-3′; *Ccl5* antisense 5′-GATGTATTCTTGAACCCACT-3′; *Cxcl10* sense 5′-ACTGCATCCATATCGATGAC-3′; *Cxcl10* antisense 5′-TTCATCGTGGCAATGATCTC-3′; *Il6* sense 5′-GTAGCTATGGTACTCCAGAAGAC-3′; *Il6* antisense 5′-ACGATGATGCACTTGCAGAA-3′. Primer sequences for *Gapdh*, *Nfkbia*, *Ifna4* and *Ifnb* are the same as those previously published[24,26].

**RNA interference.** Small interfering (si) RNA vectors were constructed by inserting oligonucleotides into *BspM*I sites of the pcPUR-U6i expression vector. The siRNA targeting sequences for murine *DAI* (*DLM-1/Zbp1*) (DAI-1 and DAI-2) and *Renilla* luciferase (control) are 5′-GGTCAAAGGGTGAAGTCAT-3′ (DAI-1), 5′-GATGAAAGAATATTAAGAT-3′ (DAI-2) and 5′-GTAGCGCGGTGTATTATACA-3′ (control), respectively. L929 cells ($1 \times 10^6$) were transfected with 2.0 μg of siRNA vector in 6.0 μl Lipofectamine2000 transfection reagent (Invitrogen). The cells were then used for subsequent assays after incubation for 48 h in the presence of puromycin (4.0 μg ml$^{-1}$; Sigma).

**EMSA.** Equal amounts, 40 μg, of whole-cell protein extract were analysed by EMSA with a $^{32}$P-radiolabelled oligonucleotide probe containing a consensus NF-κB binding sequence. The presence of p65 in the NF-κB–DNA binding complex was also confirmed by detection of a supershifted band with an anti-p65 antibody (data not shown).

**Fluorescence microscopy.** Cell culture, image acquisition and processing for the sensitized FRET were performed as described previously[25,26]. We used the following filters in this study: XF1068 and XF3079 excitation/emission filters (Omega Optical Inc.) for the YFP images; BP520-550 and BA580IF (Olympus) for rhodamine; and XF1068 and BA580IF for FRET. As a dichroic mirror, a U-MREF glass reflector (Olympus) was used. Corrected FRET (FRET$^C$) was calculated using the equation: $\mathrm{FRET}^C = \mathrm{FRET} - 0.108 \times \mathrm{YFP} - 0.194 \times \mathrm{ROX}$, where FRET, YFP and ROX represents background-subtracted images acquired through the FRET, YFP and rhodamine channels, respectively. Under our experimental condition, the fractions of the bleed-through of YFP and ROX fluorescence through the FRET channel and the bleed-through of YFP through the ROX channel were 0.176, 0.194 and 0.348, respectively.

**Pull-down assay.** Cell lysates were extracted from HEK293T cells transiently transfected with pCAGGS-HA-DAI and were first incubated for 15 min at room temperature with streptavidin-conjugated magnetic beads, and after centrifugation, the supernatants were then mixed for 20 min at 4 °C with poly(dA-dT)•poly(dT-dA), the 5′-terminal of which is unilaterally conjugated with biotin, following its pre-incubation with streptavidin-conjugated magnetic beads. The mixture was washed extensively with lysis buffer, separated by SDS–PAGE, and immunoblotted with anti-HA antibody. For the competition assay, unconjugated poly(dA-dT)•poly(dT-dA) or poly(rI:rC) was added to the binding reaction at the concentrations specified in the figure legend.

**Statistical analysis.** Differences between control and experimental groups were evaluated using the Student's *t*-test.

29. Suggs, J. W. & Wagner, R. W. Nuclease recognition of an alternating structure in a d(AT)$_{14}$ plasmid insert. *Nucleic Acids Res.* **14**, 3703–3716 (1986).
30. Braun, C. S. *et al.* The structure of DNA within cationic lipid/DNA complexes. *Biophys. J.* **84**, 1114–1123 (2003).